DOI: 10.1002/chem.201001228

Late-Transition-Metal Complexes as Tunable Lewis Bases

Jürgen Bauer, Holger Braunschweig,* Peter Brenner, Katharina Kraft, Krzysztof Radacki, and Katrin Schwab[a]

Abstract: Syntheses of the first heteroleptic N-heterocyclic carbene (NHC)–phosphane platinum(0) complexes and formation of the corresponding Lewis acid–base adducts with aluminum chloride is reported. The influence of N-heterocyclic carbenes on tuning the Lewis basic properties of the metal complexes was judged from spectroscopic, structural, and computational data. Conclusive experimental evidence for the enhanced Lewis basicity of NHC-containing complexes was provided by a transfer reaction.

Keywords: carbenes · density functional calculations · Lewis acids · Lewis bases · platinum

Introduction

The concept of Lewis basicity is of major importance in organometallic synthesis and catalysis.[1] Complexes of the type $[MX\mathbf{L}_3]$ (M = Rh, Ir; **L** = CO, PR_3), brought about by Vaska[2] and Wilkinson et al.,[3] have long been recognized as metal bases, as they constitute electron-rich, square-planar d^8 species that react readily with electrophiles and also oxidatively add, for example, H_2, R_3SiH, or R_2BH, thus rendering these complexes widely used catalysts.[4–10] Subsequently, Werner and others have developed the chemistry of Lewis basic half-sandwich complexes, for example, of the type $[(\eta^5\text{-}C_5R_5)M\mathbf{L}_2]$.[11]

Besides their importance for homogeneous catalysis, Lewis basic complexes have been employed for the synthesis of di- and oligonuclear species that display dative bonds between various metal centers. Earlier work by Pomeroy et al. reported on dinuclear species such as **1** (Scheme 1), which display a dative bond between Os and a Group 6 metal.[12–14]

It should be noted that these and related dinuclear carbonyl species, for example, **2**, display unsupported dative bonds between two different d-block metals in the crystal.

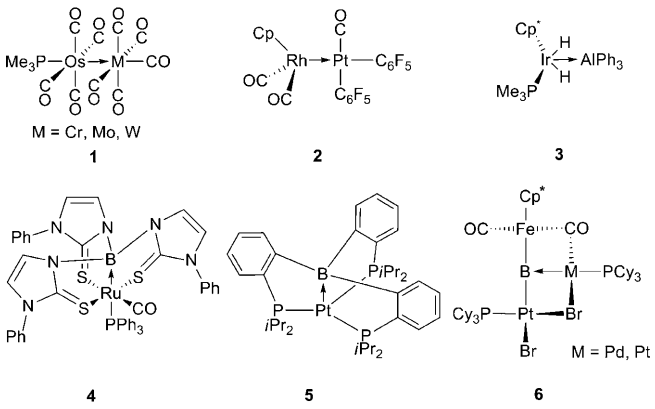

Scheme 1. Complexes **1**–**6**, which display dative bonds of Lewis basic transition-metal centers towards Lewis acidic d- and p-block metals.

However, variable temperature (VT) NMR spectroscopy revealed the presence of bridging carbonyl ligands in solution, thus supporting the dative metal–metal linkage.[15,16] Likewise, early examples of complexes with dative bonds between d- and p-block metals such as **3** generally display supported intermetal linkages.[17] Although reports on such "metal-only" Lewis pairs remained sparse and rather cursory for a long time, the field of heterodinuclear d-block/p-block complexes with dative bonds in particular has developed rapidly over the past decade. In a seminal paper from 1999, Hill et al. reported on the first metal boratrane **4** that displayed a dative Ru–B bond.[18] Subsequently, this synthetic approach has been systematically applied by Hill, Parkin, and others to the synthesis of a wide range of boratranes.[19–33]

[a] Dipl.-Chem. J. Bauer, Prof. Dr. H. Braunschweig, Dipl.-Chem. P. Brenner, Dipl.-Chem. K. Kraft, Dr. K. Radacki, Dipl.-Chem. K. Schwab
Institut für Anorganische Chemie
Julius-Maximilians-Universität Würzburg
Am Hubland, 97074 Würzburg (Germany)
Fax: (+49) 931-888-4623
E-mail: h.braunschweig@mail.uni-wuerzburg.de

Supporting information for this article is available on the WWW under http://dx.doi.org/10.1002/chem.201001228.

More recently, corresponding sila- and stannatranes have been reported that comprise supported dative bonds between d- and p-block elements.[34–36] Similarly, Bourissou et al. have successfully employed bi- and tridentate phosphanes for the synthesis of supported metal–base adducts of Group 13 elements,[37–43] and we disclosed the pronounced propensity of electron-rich metal fragments of the type [M(PR$_3$)] (M = Pd, Pt) to form dative bonds to metal-coordinated boryl and borylene ligands.[44–52] The latter species without exception display CO bridges between the metal centers and thus again supported dative metal–element bonds. Neutral Lewis pairs of the type [CpRh(PR$_3$)$_2$(AlR′$_3$)] (R = R′ = Me, Et; Cp = cyclopentadienyl) that feature unsupported transition-metal–aluminum bonds were first described by Mayer and Calabrese.[53] However, the only structurally characterized complex, [CpRh(PMe$_3$)$_2$(Al$_2$Me$_4$Cl$_2$)] (**7**), shows a significant zwitterionic contribution and was described as a cationic complex [CpRh(PMe$_3$)$_2$(AlMe$_2$)]$^+$ with a weakly associated [AlMe$_2$Cl$_2$]$^-$ counterion.

Very recently, we initiated studies on unsupported "metal-only" Lewis pairs and reported structurally characterized heterobimetallic species with Pt–M (M = Be, Al, Ga, Zr) bonds and thus representative examples for d-block/s-, p-, and d-block combinations.[54–57] For these species that are devoid of any intramolecular scaffold that supports the dative bond, the propensity of the platinum center to act as a Lewis base is apparently of vital importance. Hence, we became interested in the question of how to vary, and preferably increase, the electron-donating properties of complexes of the type [Pt**L**$_2$].

N-Heterocyclic carbenes (NHCs) have been widely applied to the process of tuning the electronic properties of transition-metal complexes. Thus NHC complexes have proven to be versatile catalysts for many important transformations such as ruthenium-catalyzed olefin metathesis, palladium-catalyzed cross-couplings, and others.[58–61]

Although Nolan et al. have performed systematic IR spectroscopic studies on the electronic effect that NHCs exert on iridium carbonyls,[62] to the best of our knowledge there has been no investigation on the direct influence of NHCs on the Lewis basic properties of the metal centers.

Herein we report on the synthesis and characterization of three new Pt^0 complexes of the general formula [(NHC)$_{(2-n)}$Pt(PCy$_3$)$_n$] (n = 0, 1; Cy = cyclohexyl) including the first heteroleptic NHC–phosphane–Pt^0 complexes, as well as a novel homoleptic NHC–Pt^0 complex. These new species were investigated with respect to their reactivity towards AlCl$_3$. From these results and on the basis of structural, spectroscopic, and computational data, the influence of NHCs towards the degree of the Lewis basicity of Pt^0 complexes was inferred.

Results and Discussion

Synthesis of NHC-containing Pt^0 complexes: The new complexes [(I*t*Bu)Pt(PCy$_3$)] (**8**; I*t*Bu = *N*,*N*′-bis(*tert*-butyl)imidazol-2-ylidene), [(SIMes)Pt(PCy$_3$)] (**9**; SIMes = *N*,*N*′-bis(mesityl)imidazolylidine), and [(SIMes)$_2$Pt] (**10**) were synthesized by ligand-exchange reactions in hexane. Since NHCs are considered to be better σ donors, and thus stronger ligands than PCy$_3$,[62,63] [Pt(PCy$_3$)$_2$] (**11**) was chosen as the starting material (Scheme 2).

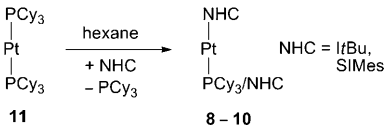

Scheme 2. Synthesis of the complexes [(I*t*Bu)Pt(PCy$_3$)] (**8**), [(SIMes)Pt(PCy$_3$)] (**9**), and [(SIMes)$_2$Pt] (**10**) by ligand exchange from the precursor [Pt(PCy$_3$)$_2$] (**11**).

The heteroleptic complexes **8** and **9** are obtained directly by stirring **11** with stoichiometric amounts of the corresponding NHC (I*t*Bu and SIMes, respectively) for 2–3.5 h at room temperature. The progress of the reaction can be monitored by ^{31}P{^{1}H} NMR spectroscopy as well by the deepening of the color from its bright original state to a dark yellow solution. The homoleptic NHC complex **10** is synthesized by adding the NHC in a twofold excess to **11** and stirring the solution at 80 °C for 18 h, whereby the color changes from bright yellow to deep orange. All three complexes are isolated by crystallization from hexane at −30 °C in good yields between 67 and 88 %. The introduction of NHCs into the ligand sphere of the platinum center results in a decrease of the ^{31}P,^{195}Pt NMR spectroscopic coupling constants (**8**: J = 3986 Hz; **9**: J = 3640 Hz) compared to the value of J = 4164 Hz found in **11**.[64]

These spectroscopic parameters provide evidence for somewhat weakened Pt–P bonds on account of the enhanced *trans* influence of the NHC ligand. Additionally, the ^{31}P{^{1}H} NMR spectroscopic resonances are slightly shifted to higher field, that is δ = 59.7 (**8**) and 58.4 ppm (**9**), respectively, versus δ = 62.3 ppm reported for **11**. Resonances of the carbenic carbon atoms in the ^{13}C{^{1}H} NMR spectra are located in the region between δ = 200 and 220 ppm, and are therefore in the expected range for late-transition-metal NHC complexes. These parameters suggest preliminary evidence for the increased electron density at the platinum center imposed by the introduction of NHCs. Additionally, the ^{195}Pt{^{1}H} NMR spectroscopic resonances all indicate, relative to the resonance of **11** (δ = −6501 ppm), a large downfield shift (δ = −6156 (**8**), −6151 (**9**), −5462 ppm (**10**); Table 1).

Single crystals of the new compounds **8**, **9**, and **10** (Figure 1) suitable for X-ray analysis were obtained by standard procedures described in the Experimental Section. All complexes display the expected overall linear geometry around the platinum center and crystallize in the space group $P\bar{1}$ (**8**, **9**) and $P2_1/n$ (**10**), respectively. As a common feature, the P-Pt-C1 and C1-Pt-C2 angles (177.2(1) (**8**), 172.4(1) (**9**), 173.9(1)° (**10**)) are considerably wider than the P1-Pt-P2 angle of 160.5(2)° in **11**, thus indicating a some-

Table 1. NMR spectroscopic parameters of compounds **8**–**11**.

Compound	^{31}P[a]	$^{1}J(P,Pt)$[b]	^{13}C[a]	^{195}Pt[a]
11	62.3	4164	–	−6501
8	59.7	3986	201.2	−6156
9	58.4	3640	216.9	−6151
10	–	–	215.9	−5462

[a] δ in ppm. [b] ^{1}J coupling constant in Hz. Data for **11** from ref. [65].

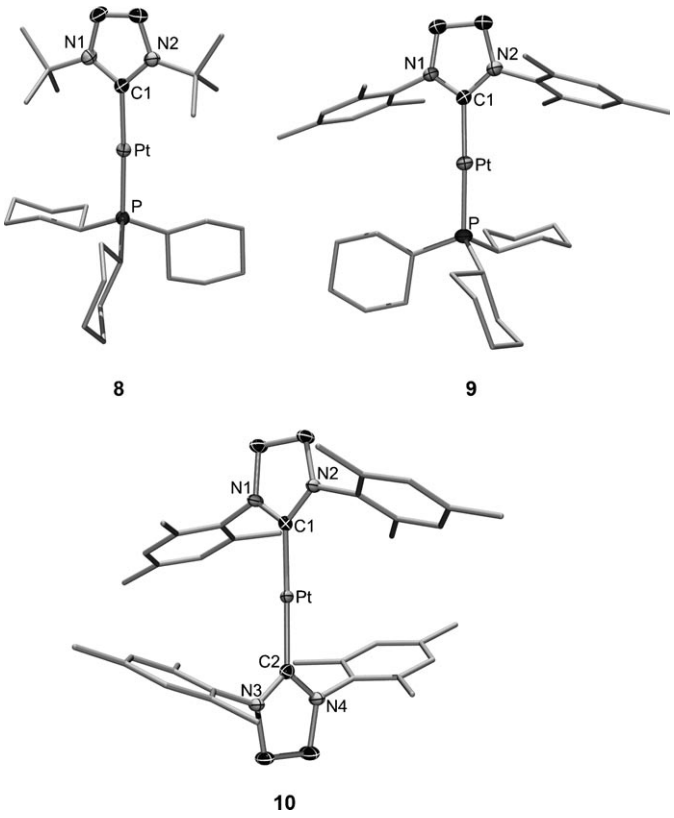

Figure 1. Molecular structures of **8**, **9**, and **10**. Relevant bond lengths [Å] and angles [°]: **8**: Pt–C1 2.027(3), Pt–P 2.211(1), C1-Pt-P 177.2(1); **9**: Pt–C1 1.991(2), Pt–P 2.228(1), C1-Pt-P 172.4(1); **10**: Pt–C1 1.959(2), Pt–C2 1.974(2), C1-Pt-C2 173.9(1) Ellipsoids are drawn at the 50% probability level. Ellipsoids of the ligands, solvent molecules, and hydrogen atoms are omitted for clarity.

what smaller deviation from linearity (Table 2). Despite all aforementioned NMR spectroscopic evidence for a pronounced *trans* influence of the NHC ligands in solution, the P–Pt distances in **8** and **9** are rather unobtrusive and do not differ much from those in **11**. It should be noted, though, that a similar finding can be drawn from the comparison of the few structural data that are available for corresponding palladium complexes. Thus, the Pd–P separation in the corresponding $[Pd(PCy_3)_2]$ complex (**12**), which also shows a P1-metal-P2 angle of 158°, was found to be 2.26 Å.[66]

The corresponding heteroleptic NHC complex [(IPr)Pd-(PCy_3)] (**13**) displays a C1-Pd-P angle of 170.88(2)° and a Pd–P distance of 2.2212(3) Å,[67] and thus a corresponding trend in structural data.

Synthesis of Lewis acid–base adducts: The T-shaped Lewis acid–base adducts $[(I\mathit{t}Bu)(Cy_3P)Pt(AlCl_3)]$ (**8′**), $[(SIMes)(Cy_3P)Pt(AlCl_3)]$ (**9′**), and $[(SIMes)_2Pt(AlCl_3)]$ (**10′**) are obtained by stirring the precursors **8**, **9**, and **10** in benzene at ambient temperature with equimolar amounts of $AlCl_3$ (Scheme 3).

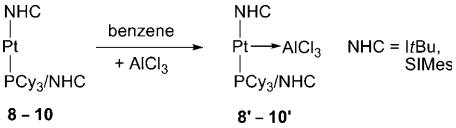

Scheme 3. Syntheses of the complexes $[(I\mathit{t}Bu)(Cy_3P)Pt(AlCl_3)]$ (**8′**), $[(SIMes)(Cy_3P)Pt(AlCl_3)]$ (**9′**), and $[(SIMes)_2Pt(AlCl_3)]$ (**10′**).

The constitution of the alane complexes in solution is indicated by multinuclear NMR spectroscopic data, in particular by $^{31}P\{^{1}H\}$ NMR spectroscopy. The corresponding resonances of the heteroleptic adducts **8′** ($\delta = 39.1$ ppm) and **9′** ($\delta = 45.5$ ppm; Table 3) show a significant high-field shift in comparison to those of the precursors **8** ($\delta = 59.7$ ppm) and **9** ($\delta = 58.4$ ppm). A similar, albeit somewhat less notable trend was found for **11** ($\delta = 62.3$ ppm) and its corresponding alane adduct $[(Cy_3P)_2Pt(AlCl_3)]$ (**11′**, $\delta = 53.5$ ppm). Likewise the $^{31}P,^{195}Pt$ NMR coupling constants are significantly reduced to $J = 2915$ (**8′**) and 2875 Hz (**9′**) relative to those of the starting materials **8** ($J = 3986$ Hz) and **9** ($J = 3640$ Hz). This is again in good agreement with the observed decrease in the coupling constant to $J = 3032$ Hz (**11′**) upon alane adduct formation of **11** ($J = 4164$ Hz). These $^{31}P\{^{1}H\}$ NMR spectroscopic data provide some evidence for a decreased platinum–phosphorus interaction in the alane adducts with respect to the platinum complex precursors, presumably brought about by electron donation through the d_{z^2} orbital[68] to the Lewis acid, and more importantly, by the increased coordination number of the platinum centers. A similar situation can be found for the $^{13}C\{^{1}H\}$ NMR spectroscopic res-

Table 2. Structural parameters of compounds **8**–**11**.

Compound	C–Pt[a]	P–Pt[a]	L-Pt-L[b]
11	–	2.231(4) 2.231(4)	160.5(2)
8	2.027(3)	2.211(1)	177.2(1)
9	1.991(2)	2.228(1)	172.4(1)
10	1.959(2) 1.974(2)	–	173.9(1)

[a] Distance [Å]. [b] Angle [°]. Data for **11** from ref. [65].

Table 3. NMR spectroscopic parameters of compounds **8′**–**11′**.

Compound	^{31}P[a]	$^{1}J(P,Pt)$[b]	^{13}C[a]
11′	53.5	3032	–
8′	39.1	2915	188.7
9′	45.5	2875	213.7
10′	–	–	211.2

[a] δ in ppm. [b] ^{1}J coupling constant in Hz. Data for **11′** from ref. [65].

onances of the carbenic carbon atoms. Here, upon adduct formation the corresponding resonances shift slightly to higher field from $\delta = 216.9$ (**9**) and 215.9 ppm (**10**) to $\delta =$ 213.7 (**9′**) and 211.2 ppm (**10′**). A more significant effect was observed for the adduct **8′** ($\delta = 188.7$ ppm) in comparison to its precursor **8** ($\delta = 201.2$ ppm).

Due to the large quadrupolar momentum of aluminum,[69] it is not possible to apply $^{195}Pt\{^{1}H\}$ NMR spectroscopy to compare the resonances of the Pt^0 complexes with their corresponding Lewis acid–base adducts (Table 3)

Single crystals of the alane complexes **8′**, **9′**, and **10′** (Figure 2) suitable for X-ray analysis were obtained by standard procedures as described in the Experimental Section. The complexes crystallize in the space group $P2_1/n$ (**8′**), $Pna2_1$ (**9′**), and $P2_1/c$ (**10′**), respectively, and, as a common feature, exhibit a T-shaped coordination geometry of the platinum center, as already observed for the neutral compound $[(Cy_3P)_2Pt(AlCl_3)]$ (**11′**)[54] and the cationic Pt^{II} complex $[(Cy_3P)_2Pt(BBr_2)][BAr^f_4]$ **14** ($Ar^f = 3,5\text{-}(CF_3)_2C_6H_3$).[70]

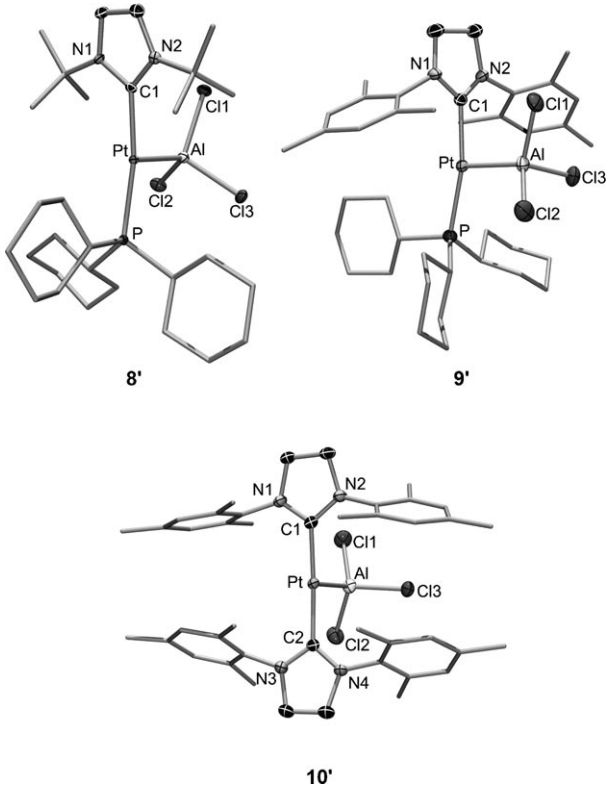

Figure 2. Molecular structures of **8′**, **9′**, and **10′**. Relevant bond lengths [Å] and angles [°]: **8′**: Pt–C1 2.040(4), Pt–P 2.295(2), Pt–Al 2.398(2), Al–Cl1 2.167(2), Al–Cl2 2.170(2), Al–Cl3 2.170(2), C-Pt-P 163.9(2), C-Pt-Al 94.6(2), P-Pt-Al 101.6(1), Cl1-Al-Cl2 105.1(1), Cl1-Al-Cl3 106.1(1), Cl2-Al-Cl3 106.0(1), Cl3-Al–Pt 110.1(1); **9′**: Pt–C 1.991(9), Pt–P 2.301(2), Pt–Al 2.384(2), Al–Cl1 2.147(2), Al–Cl2 2.157(2), Al–Cl3 2.172(2), C-Pt-P 168.3(5), C-Pt-Al 88.5(5), P-Pt-Al 103.1(1), Cl1-Al-Cl2 107.7(1), Cl1-Al-Cl3 106.6(1), Cl2-Al-Cl3 102.5(1), Cl1-Al-Pt 112.4(1); **10′**: Pt–C 2.021(2), Pt–C′ 2.037(2), Pt–Al 2.370(1), Al–Cl1 2.142(1), Al–Cl2 2.165(1), Al–Cl3 2.158(1), C-Pt-C′ 174.6(1), C-Pt-Al 90.9(1), C′-Pt-Al 94.5(1), Cl1-Al-Cl2 106.0(1), Cl1-Al-Cl3 108.3(1), Cl2-Al-Cl3 103.4(1), Cl1-Al-Pt 110.5(1). Ellipsoids are drawn at the 50% probability level. Ellipsoids of the ligands and hydrogen atoms are omitted for clarity.

The Pt–P and Pt–C bond lengths are elongated due to the increased coordination number of platinum (Table 4). For example, the P–Pt distance found in **8′** (2.295(2) Å) is relative to **8** (2.211(1) Å), increased by 3.8%. This is in good agreement with the increase found in the known species **11** and **11′** (3.0 and 3.5%, respectively). Likewise, the aluminum atoms in all new adducts display the expected slightly distorted tetrahedral geometry already found for **11′**, and the Pt–Al separations deviate only 0.1–0.7% from the one reported for **11′** (Table 4). Interestingly, complex **10′** reveals an almost coplanar mutual orientation of the two SIMes groups, whereas the ligands in the starting material **10** show an orthogonal arrangement.

Table 4. Structural parameters of compounds **8′**–**11′**.

Compound	C–Pt[a]	P–Pt[a]	Al–Pt[a]	L-Pt-L[b]
11′	–	2.299(1) 2.313(1)	2.386(1)	162.1(1)
8′	2.040(4)	2.295(2)	2.398(2)	163.9(2)
9′	1.991(9)	2.301(2)	2.384(2)	168.3(5)
10′	2.021(2) 2.037(2)	–	2.370(1)	174.6(1)

[a] Distance [Å]. [b] Angle [°]. Data for **11′** from ref. [65].

Some of the aforementioned spectroscopic and structural data seem to suggest a somewhat enhanced electron density and thus Lewis basicity of the platinum centers in **8**–**10** brought about by the introduction of ligands with a strong *trans* influence, that is the NHCs.

Density functional theory (DFT) calculations: To provide further information about the influence of NHCs on the Lewis basicity of the title compounds towards $AlCl_3$, DFT calculations were carried out (Scheme 4).[71]

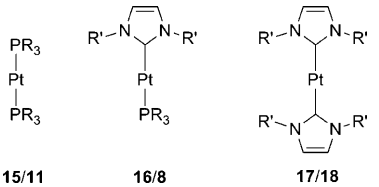

Scheme 4. Models used for the DFT calculations: **15**–**17**: R = R′ = Me; **11**, **8**, **18**: R = Cy, R′ = *t*Bu.

The optimized structures of $[Pt(PMe_3)_2]$ (**15**), $[(IMe)Pt(PMe_3)]$ (**16**), and $[(IMe)_2Pt]$ (**17**) were calculated to determine the influence of the steric hindrance in the investigated systems. These compounds serve as simplified models for the complexes $[Pt(PCy_3)_2]$ (**11**), $[(I\mathit{t}Bu)Pt(PCy_3)]$ (**8**), and $[(I\mathit{t}Bu)_2Pt]$ (**18**).

In addition, the corresponding alane adducts of both original and simplified compounds were optimized using the same methods ($[(Me_3P)_2Pt(AlCl_3)]$ (**15′**), $[(IMe)(Me_3P)Pt(AlCl_3)]$ (**16′**), $[(IMe)_2Pt(AlCl_3)]$ (**17′**), $[(Cy_3P)_2Pt(AlCl_3)]$

(**11′**), [(I*t*Bu)(Cy_3P)Pt($AlCl_3$)] (**8′**), and [(I*t*Bu)$_2$Pt($AlCl_3$)] (**18′**), respectively).

The computed geometries show similar structural parameters to those derived from the experiments. However, the calculated distances are slightly overestimated (by approximately 1.2–3.5 %). The C–Pt distances are longer by 3.4 (**8**) and 2.5 pm (**8′**), and the P–Pt distances by 7.7 (**8**) and 7.3 pm (**8′**).

The SCF energies of all optimized compounds were used to determine the bonding dissociation enthalpies (BDEs) for the alane adducts. As expected, the strength of the Pt–Al bond increases as the phosphane ligands are consecutively replaced by NHCs.

Therefore, the BDE increases along the series **15′** (-162 kJ mol^{-1}) < **16′** (-188 kJ mol^{-1}) < **17′** (-204 kJ mol^{-1}). Interestingly, this trend is different for the unsimplified compounds: **18′** (-121 kJ mol^{-1}) < **11′** (-141 kJ mol^{-1}) < **8′** (-157 kJ mol^{-1}) (Table 5). Nonetheless, even the smallest calculated platinum alane interaction surpasses those determined for transition-metal alane adducts of the type [CpRh(PR_3)$_2$(AlR'_3)] (R = R′ = Me, Et) (75 kJ mol^{-1}) by about 45 kJ mol^{-1}.[53]

Table 5. Selected calculated geometrical and electronic parameters of [L_2Pt($AlCl_3$)].

	11′	**8′**	**18′**	**15′**	**16′**	**17′**
Pt–Al [Å]	2.458	2.455	2.477	2.467	2.451	2.441
WBI[a] (Pt–Al)	0.52	0.55	0.57	0.51	0.54	0.57
WBI[a] (Pt–L1)	0.50	0.51	0.53	0.52	0.53	0.54
WBI[a] (Pt–L2)	0.50	0.51	0.50	0.51	0.53	0.54
natural charge						
Pt	−0.31	−0.22	−0.13	−0.34	−0.26	−0.17
Al	1.32	1.29	1.28	1.31	1.30	1.29
BDE [kJ mol^{-1}]	−141	−157	−121	−162	−188	−204
ΔE_{prep}[b] (Pt**L**$_2$)	39.8	43.8	78.9	15.6	8.4	13.2
ΔE_{prep}[b] ($AlCl_3$)	98.5	101.4	113.3	84.3	86.0	92.5
ΔE_{int}[c] (Pt–Al)	−279.5	−302.2	−313.2	−261.8	−282.3	−309.5
	11	**8**	**18**	**15**	**16**	**17**
WBI[a] (Pt–**L1**)	0.59	0.63	0.62	0.61	0.64	0.65
WBI[a] (Pt–**L2**)	0.59	0.58	0.62	0.61	0.62	0.65
natural charge						
Pt	−0.48	−0.40	−0.32	−0.53	−0.47	−0.40

[a] Wiberg bond index. [b] Preparation energy in kJ mol^{-1}. [c] Interaction energy in kJ mol^{-1} (**L1**, **L2** = PR_3, NHC).

This unexpected deviation in the case of the sterically encumbered **18′** can be rationalized by higher preparation energies for both reaction partners when compared with the sterically less crowded complexes **11′** and **8′**. The bulky I*t*Bu ligand causes stronger distortion of the $AlCl_3$ moiety in **18′**, which leads to higher ΔE_{prep} for the alane (about 10 kJ mol^{-1} higher than in the case of **11′** and **8′**). Even more essential for the observed trend in BDEs is the ΔE_{prep} of the T-shaped metal fragments. As mentioned above, the two NHC ligands in homoleptic complexes such as **18** are mutually orthogonal, whereas the alane adducts reveal a more eclipsed arrangement. Thus, rotation of the NHCs about the C1-Pt-C2 axis significantly contributes to ΔE_{prep} in **18**, and accordingly this rotational barrier was calculated to be 36 kJ mol^{-1}. In the case of the simplified complex **17**, the NHC rotational barrier amounts only to 5 kJ mol^{-1}. The significant differences in ΔE_{prep} are therefore held responsible for the observed deviation from the expected trend for the unsimplified complexes compared to the simplified model species.

The degree of orbital interactions has been estimated using the natural bond orbital (NBO) method.[72–75] Decrease in the natural charge of the platinum centers is observed as NHC ligands are gradually introduced (-0.31 (**11**) to -0.13 (**8**) and -0.34 (**15**) to -0.17 (**17**), respectively), thereby providing evidence for the superior π-acceptor properties of NHCs compared to phosphanes.[76,77] Evidence for the strengthening of the Pt–Al interaction through ligand substitution is also provided by an increased Pt–Al Wiberg bond index (WBI) as NHC ligands are added (0.52 (**11′**), 0.55 (**8′**), 0.57 (**18′**), 0.51 (**15′**), 0.54 (**16′**), 0.57 (**17′**)).

Additionally, the WBIs between the donor ligands and the platinum center in the alane adducts are lowered by 0.07–0.12 in comparison to the starting complexes (Table 5), which is in accordance with their crystallographically observed and computationally determined elongated bond lengths.

As expected, the natural charges of the platinum centers in the adducts are slightly more positive by approximately 0.20 *e*, and accordingly those of the aluminum atoms are more negative by the same amount relative to those of the starting materials PtL_2 and $AlCl_3$. Therefore, although the T-shaped structures of the alane adducts reveal similarities with the cationic complex [(Cy_3P)$_2$Pt(BBr_2)][BAr^f_4] (**14**), the calculations suggest a practically neutral platinum center.

Transfer of the Lewis acid $AlCl_3$: Based on the aforementioned computations, in particular the high BDE for the dative Pt–Al bond and the favorably low ΔE_{prep}, the new heteroleptic complex **8** appears to exhibit an enhanced propensity to act as Lewis base towards $AlCl_3$ in comparison to the homoleptic species.

To provide conclusive experimental evidence for this assumption, a transfer experiment was carried out. To this end, [(Cy_3P)$_2$Pt($AlCl_3$)] (**11′**) was dissolved in benzene at ambient temperature and treated with an equimolar amount of [(I*t*Bu)Pt(PCy_3)] (**8**) (Scheme 5).

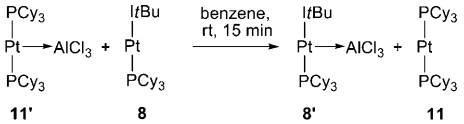

11′ **8** **8′** **11**

Scheme 5. Transfer of the $AlCl_3$ fragment from [(Cy_3P)$_2$Pt($AlCl_3$)] (**11′**) to [(I*t*Bu)Pt(PCy_3)] (**8**).

Monitoring the reaction mixture by multinuclear NMR spectroscopy indeed revealed complete transfer of the Lewis acid $AlCl_3$ from **11′** to **8** with formation of the adduct

[(I*t*Bu)(Cy_3P)Pt($AlCl_3$)] (**8′**) (vide supra). $^{31}P\{^1H\}$ NMR spectra of the reaction mixture revealed a gradual decrease of the signals at $\delta = 53.5$ (**11′**) and 59.7 ppm (**8**), respectively, which are associated with the starting materials, with concomitant increase of the product signals at $\delta = 62.3$ (**11**) and 39.1 ppm (**8′**). The transfer was complete after 15 min at ambient temperature and proceeded without formation of soluble side or degradation products as judged by multinuclear NMR spectroscopy.

Additionally, the transfer reaction of the homoleptic NHC–Pt adduct **10′** towards the stronger Lewis base **8** was carried out. In comparison with the above-mentioned transfer experiment, this reaction requires higher temperatures (80 °C in comparison to room temperature) and extended reaction times (about 70 % conversion after 60 h, as determined by NMR spectroscopy). Additionally, due to the harsher reaction conditions, degradation products are formed. In particular, after heating for more than 60 h, the formation of the degradation products increases significantly. However, the results clearly indicate that the heteroleptic adduct **8′** is favored over the homoleptic adducts **10′** and **11′**.

Conclusion

The first heteroleptic NHC–phosphane complexes and a new homoleptic NHC complex of Pt^0 were prepared and fully characterized in solution and in the solid state, together with their corresponding $AlCl_3$ adducts. The description of the bonding mode in these adducts based on experimental and computational data fulfills criteria previously defined by Hill et al.[18] and Parkin et al.[26] for metal borane adducts. Both the experimental and the computational data are consistent with a dative bond between aluminum and platinum.

The influence of NHCs on the Lewis basicity of the platinum centers was assessed on the basis of spectroscopic and structural data as well as DFT calculations. In particular, the latter gave evidence for a correlation between the number (and type) of NHC ligands and the strength of the dative Pt–Al interaction as judged by the corresponding BDE. Conclusive experimental evidence for the prediction that NHCs enhance the Lewis basicity of Pt^0 centers was brought about by a transfer reaction between [(Cy_3P)$_2$Pt($AlCl_3$)] (**11′**) and the presumed stronger base [(I*t*Bu)Pt(PCy_3)] (**8**), which led to quantitative formation of [(I*t*Bu)(Cy_3P)Pt($AlCl_3$)] (**8′**).

Experimental Section

General considerations: All manipulations were performed either under an atmosphere of dry argon or in vacuo using standard Schlenk line and glovebox techniques. Solvents were purified by distillation under dry argon from sodium and stored under argon over molecular sieves. NMR spectra were acquired using Bruker AMX 400 (^1H: 400.1 MHz, $^{13}C\{^1H\}$: 100.6 MHz, $^{31}P\{^1H\}$: 162.0 MHz) or Bruker Avance 500 (^1H: 500.1 MHz, $^{13}C\{^1H\}$: 125.8 MHz, ^{15}N: 50.7 MHz, $^{31}P\{^1H\}$: 202.5 MHz, $^{195}Pt\{^1H\}$: 106.9 MHz) NMR spectrometers. ^1H and ^{13}C NMR spectra were referenced to external TMS through the residual protons of the solvent (^1H) or the solvent itself (^{13}C). ^{15}N NMR spectra were referenced to external nitromethane, ^{31}P NMR spectra were referenced to external H_3PO_4 (85 %), and ^{195}Pt NMR spectra were referenced to $Na_2[PtCl_6]$ in D_2O.

Synthesis of [(I*t*Bu)Pt(PCy_3)] (8): In a 50 mL Schlenk flask, [Pt(PCy_3)$_2$] (**11**) (300 mg, 0.40 mmol) and I*t*Bu (80.0 mg, 0.44 mmol) were dissolved in hexane (10 mL) and stirred for 2 h at room temperature. After cooling the solution to −30 °C for 24 h, the solvent was decanted and the residue dried in vacuo to yield **8** as a bright yellow solid (230 mg, 0.35 mmol, 88 %). Crystals suitable for X-ray diffraction were grown from a solution in hexane at −30 °C. ^1H NMR (400.1 MHz, C_6D_6): $\delta = 6.56$ (s, 2H; NC*HCH*N), 2.44–2.35 (m, 6H; Cy), 2.09 (s, 18H; C(CH_3)$_3$), 1.99–1.25 ppm (m, 27H; Cy); $^{13}C\{^1H\}$ NMR (100.6 MHz, C_6D_6): $\delta = 201.2$ (d, ^2J(C,P) = 121 Hz; N*C*N), 113.9 (d, ^4J(C,P) = 4 Hz; N*CH*C*H*N), 58.3 (s; *C*(CH_3)$_3$), 36.2 (d, ^1J(C,P) = 24 Hz; Cy), 32.1 (s; C(*CH*$_3$)$_3$), 31.8 (d, ^3J(C,P) = 3 Hz, Cy), 28.2 (d, ^2J(C,P) = 10 Hz; Cy), 27.4 ppm (s; Cy); ^{15}N NMR (50.7 MHz, C_6D_6): $\delta = -170$ ppm; $^{31}P\{^1H\}$ NMR (162.0 MHz, C_6D_6): $\delta = 59.7$ ppm (^1J(P,Pt) = 3986 Hz); $^{195}Pt\{^1H\}$ NMR (106.9 MHz, C_6D_6): $\delta = -6156$ ppm (^1J(Pt,P) = 3965 Hz); elemental analysis calcd (%) for $C_{29}H_{53}N_2PPt$: C 53.11, H 8.15, N 4.27; found: C 53.50, H 8.23, N 4.45.

Synthesis of [(SIMes)Pt(PCy_3)] (9): [Pt(PCy_3)$_2$] (**11**) (200 mg, 0.26 mmol) and SIMes (89.0 mg, 0.26 mmol) were dissolved in hexane (10 mL) in a 50 mL Schlenk flask and stirred for 3.5 h at room temperature. After cooling the solution to −30 °C for 30 h, the solvent was decanted and the residue dried in vacuo to yield **9** as a dark yellow solid (140 mg, 0.18 mmol, 69 %). Crystals suitable for X-ray diffraction were grown from a solution in hexane at −30 °C. ^1H NMR (500.1 MHz, C_6D_6): $\delta =$ 6.87 (s, 4H; *H*(ar.)), 3.12 (s, 4H; NC*H*$_2$C*H*$_2$N), 2.52 (s, 12H; *o*-C*H*$_3$), 2.21 (s, 6H; *p*-C*H*$_3$), 1.94–1.13 ppm (m, 33H; Cy); $^{13}C\{^1H\}$ NMR (125.7 MHz, C_6D_6): $\delta = 216.9$ (d, ^2J(C,P) = 115 Hz; N*C*N), 137.3 (s; *C*(ar.)), 135.2 (s; *C*(ar.)), 134.9 (s; *C*(ar.)), 126.9 (s; *C*(ar.)), 48.5 (s; N*C*H$_2$*C*H$_2$N), 34.2 (d; ^1J(C,P) = 23 Hz; Cy), 30.6 (d, ^3J(C,P) = 3 Hz; Cy), 26.5 (d, ^{2}J(C,P) = 11 Hz; Cy), 25.7 (s; Cy), 19.8 (s; *p*-*C*H$_3$), 17.5 ppm (s; *o*-*C*H$_3$); ^{15}N NMR (50.7 MHz, C_6D_6): $\delta = -252$ ppm; $^{31}P\{^1H\}$ NMR (202.5 MHz, C_6D_6): $\delta =$ 58.4 ppm (^1J(P,Pt) = 3640 Hz); $^{195}Pt\{^1H\}$ NMR (106.9 MHz, C_6D_6): $\delta =$ −6151 ppm (^1J(Pt,P) = 3634 Hz); elemental analysis calcd (%) for $C_{39}H_{59}N_2PPt$: C 59.90, H 7.61, N 3.58; found: C 59.62, H 7.61, N 3.82.

Synthesis of [(SIMes)$_2$Pt] (10): In a 50 mL Schlenk flask, [Pt(PCy_3)$_2$] (**11**) (200 mg, 0.26 mmol) and SIMes (160 mg, 0.53 mmol, 2 equiv) were dissolved in hexane (15 mL) and stirred for 18 h at 80 °C. After cooling the solution to −30 °C for 48 h, the solvent was decanted and the residue dried in vacuo to yield **10** as an orange-yellow solid (140 mg, 0.17 mmol, 67 %). Crystals suitable for X-ray diffraction were grown by means of diffusion of hexane to a benzene solution at room temperature. ^1H NMR (500.1 MHz, C_6D_6): $\delta = 6.85$ (s, 8H; *H* (ar.)), 2.90 (s, 8H; NC*H*$_2$C*H*$_2$N), 2.34 (s, 12H; *p*-C*H*$_3$), 2.14 ppm (s, 24H; *o*-C*H*$_3$); $^{13}C\{^1H\}$ NMR (125.7 MHz, C_6D_6): $\delta = 215.9$ (s; N*C*N), 139.0 (s; *C*(ar.)), 136.6 (s; *C*(ar.)), 135.3 (s; *C*(ar.)), 128.8 (s; *C*(ar.)), 49.7 (s; N*C*H$_2$*C*H$_2$N), 21.3 (s; *p*-*C*H$_3$), 18.7 ppm (s; *o*-*C*H$_3$); ^{15}N NMR (30.4 MHz, C_6D_6): $\delta = -254$ ppm; $^{195}Pt\{^1H\}$ NMR (106.9 MHz, C_6D_6): $\delta = -5462$ ppm; elemental analysis calcd (%) for $C_{45}H_{52}N_4Pt$: C 62.43, H 6.49, N 6.93; found: C 62.28, H 6.49, N 7.55.

Synthesis of [(I*t*Bu)(Cy_3P)Pt($AlCl_3$)] (8′): In a J. Young NMR tube, **8** (15.0 mg, 23.0 μmol) and $AlCl_3$ (5.0 mg, 48.0 μmol) were dissolved in C_6D_6 (0.6 mL). After 1 d at room temperature, a yellow precipitate appeared. Recrystallization yielded **8′** (8.1 mg, 10.3 μmol, 68 %). Crystals suitable for X-ray diffraction were grown by means of diffusion of hexane to a benzene solution at room temperature. ^1H NMR (500.1 MHz, C_6D_6): $\delta = 6.59$ (s, 2H; NC*HCH*N), 2.40–2.28 (m, 3H; Cy), 2.10–2.04 (m, 6H; Cy), 1.82 (s, 18H; C(*CH*$_3$)$_3$), 1.80–1.72 (m, 12H; Cy), 1.64–1.56 (m, 6H; Cy), 1.35–1.23 ppm (m, 6H; Cy); $^{13}C\{^1H\}$ NMR (125.7 MHz, C_6D_6): $\delta = 188.7$ (d, ^2J(C,P) = 109 Hz; N*C*N), 117.9 (s; N*CH*C*H*N), 59.5 (s; *C*(CH_3)$_3$), 34.6 (d, ^1J(C,P) = 26 Hz; Cy), 32.8 (s; C(*CH*$_3$)$_3$), 30.9 (s; Cy), 27.7 (d, ^2J(C,P) = 10 Hz; Cy), 26.4 ppm (s; Cy); $^{31}P\{^1H\}$ NMR (202.5 MHz, C_6D_6): $\delta = 39.1$ ppm (^1J(P,Pt) = 2915 Hz); elemental analysis calcd (%) for $C_{29}H_{53}AlCl_3N_2PPt$: C 44.14, H 6.77, N 3.55; found: C 43.31, H 6.64, N 4.19.

Synthesis of [(SIMes)(Cy_3P)Pt($AlCl_3$)] (9′): In a J. Young NMR tube, **9** (10.0 mg, 13.0 μmol) and $AlCl_3$ (1.7 mg, 13.0 μmol) were dissolved in C_6D_6 (0.6 mL). After 1 d at room temperature, yellow crystals were formed. Recrystallization yielded **9′** (7.4 mg, 8.1 μmol, 62%). Crystals suitable for X-ray diffraction were grown from a solution in toluene at −30°C. ^{1}H NMR (500.1 MHz, C_6D_6): δ = 6.90 (s, 2H; *H*(ar.)), 6.67 (s, 2H; *H*(ar.)), 3.46–3.43 (m, 2H; NCH_2CH_2N), 2.96–2.92 (m, 2H; NCH_2CH_2N), 2.75 (s, 6H; CH_3), 2.30 (s, 6H; CH_3), 2.14 (s, 6H; CH_3), 1.82–1.14 ppm (m, 33H; Cy); ^{13}C{^{1}H} NMR (125.7 MHz, C_6D_6): δ = 213.7 (d, ^2J(C,P) = 104 Hz; N*C*N), 138.5 (s; *C*(ar.)), 137.8 (s; *C*(ar.)), 136.3 (s; *C*(ar.)), 134.5 (s; *C*(ar.)), 131.0 (s; *C*(ar.)), 128.7 (s; *C*(ar.)), 51.6 (s; NCH_2CH_2N), 51.6 (s; NCH_2CH_2N), 35.1 (d, ^1J(C,P) = 26 Hz; Cy), 30.9 (s; Cy), 27.7 (d, ^2J(C,P) = 11 Hz; Cy), 23.0 (s; Cy), 20.9 (s; *p*-CH_3), 20.6 (s; *o*-CH_3), 20.5 ppm (s; *o*-CH_3); ^{31}P{^{1}H} NMR (202.5 MHz, C_6D_6): δ = 45.5 ppm (^1J(P,Pt) = 2875 Hz); elemental analysis calcd (%) for $C_{39}H_{59}AlCl_3N_2PPt$: C 51.18, H 6.50, N 3.06; found: C 50.76, H 6.43, N 3.08.

Synthesis of [($(SIMes)_2$Pt($AlCl_3$)] (10′): In a J. Young NMR tube, **10** (10.0 mg, 12.4 μmol) and $AlCl_3$ (1.7 mg, 12.4 μmol) were dissolved in C_6D_6 (0.6 mL). After 3 d at room temperature, an orange precipitate appeared. Recrystallization yielded **10′** (6.8 mg, 7.2 mmol, 58%). Crystals suitable for X-ray diffraction were grown from a solution in hexane at −30°C. ^{1}H NMR (500.1 MHz, C_6D_6): δ = 6.67 (s, 8H; *H*(ar.)), 2.98 (s, 8H; NCH_2CH_2N), 2.33 (s, 24H; *o*-CH_3), 2.26 ppm (s, 12H; *p*-CH_3); ^{13}C{^{1}H} NMR (125.7 MHz, C_6D_6): δ = 211.2 (s; N*C*N), 137.2 (s; *C*(ar.)), 136.6 (s; *C*(ar.)), 135.9 (s; *C*(ar.)), 128.3 (s; *C*(ar.)), 51.8 (s; NCH_2CH_2N), 21.4 (s; *p*-CH_3), 20.7 ppm (s; *o*-CH_3); elemental analysis calcd (%) for $C_{42}H_{52}AlCl_3N_4Pt$: C 53.59, H 5.57, N 5.95; found: C 53.58, H 5.60, N 5.65.

Crystal structure determination: The crystal data of **10** and **8′** were collected using a Bruker X8 APEX diffractometer with multilayer mirror monochromated $Mo_{K\alpha}$ radiation, and those of **8**, **9**, **9′**, and **10′** were collected using a Bruker SMART APEX with graphite-monochromated $Mo_{K\alpha}$ radiation. Both diffractometers were equipped with CCD area detectors. The structures were solved using direct methods, refined with the SHELX software package[78] and expanded using Fourier techniques. All non-hydrogen atoms were refined anisotropically. Hydrogen atoms were assigned to idealized positions and were included in structure-factors calculations.

Crystal data for 8: $C_{29}H_{53}N_2PPt$; M_r = 655.79; colorless block; 0.29 × 0.22 × 0.08 mm^3; triclinic; space group $P\bar{1}$; a = 9.3236(10), b = 9.7329(14), c = 18.541(2) Å; α = 93.719(2), β = 93.301(2), γ = 118.4350(10)°; V = 1468.9(3) Å^3; Z = 2; ρ_{calcd} = 1.483 g cm^{-3}; μ = 4.849 mm^{-1}; $F(000)$ = 668; T = 174(2) K; R_1 = 0.0299, wR^2 = 0.0667, 7332 independent reflections ($2\theta \leq 56.84°$) and 304 parameters.

Crystal data for 9: $C_{39}H_{59}N_2PPt{\cdot}C_6H_{14}$; M_r = 868.11; yellow block; 0.17 × 0.29 × 0.43 mm^3; triclinic; space group $P\bar{1}$; a = 12.728(3), b = 13.091(3), c = 15.419(3) Å; α = 111.647(3), β = 96.942(3), γ = 108.799(3)°; V = 2175.1(8) Å^3; Z = 2; ρ_{calcd} = 1.325 g cm^{-3}; μ = 3.293 mm^{-1}; $F(000)$ = 900; T = 174(2) K; R_1 = 0.0286, wR^2 = 0.0683, 10833 independent reflections ($2\theta \leq 5670°$) and 470 parameters.

Crystal data for 10: $C_{42}H_{52}N_4Pt$; M_r = 807.97; yellow block; 0.09 × 0.12 × 0.23 mm^3; monoclinic; space group $P2_1/n$; a = 17.0311(14), b = 10.3805(9), c = 21.5737(17) Å; α = 90.00, β = 99.008(2), γ = 90.00°; V = 3767.0(5) Å^3; Z = 4; ρ_{calcd} = 1.425 g cm^{-3}; μ = 3.758 mm^{-1}; $F(000)$ = 1640; T = 100(2) K; R_1 = 0.0193, wR^2 = 0.0413, 7400 independent reflections ($2\theta \leq 52.22°$) and 436 parameters.

Crystal data for 8′: $C_{29}H_{53}AlCl_3N_2PPt$; M_r = 791.14; yellow plate; 0.07 × 0.22 × 0.26 mm^3; monoclinic; space group $P2_1/n$; a = 10.035(6), b = 17.851(11), c = 18.867(12) Å; α = 90.00, β = 98.678(9), γ = 90.00°; V = 3341(4) Å^3; Z = 4; ρ_{calcd} = 1.573 g cm^{-3}; μ = 4.535 mm^{-1}; $F(000)$ = 1600; T = 100(2) K; R_1 = 0.0365, wR^2 = 0.0819, 7949 independent reflections ($2\theta \leq 56.5°$) and 340 parameters.

Crystal data for 9′: $C_{39}H_{59}AlCl_3N_2PPt$; M_r = 915.27; yellow plate; 0.35 × 0.29 × 0.08 mm^3; orthorhombic; space group $Pna2_1$; a = 20.422(4), b = 17.716(4), c = 11.445(2) Å; V = 4140.9(15) Å^3; Z = 4; ρ_{calcd} = 1.468 g cm^{-3}; μ = 3.670 mm^{-1}; $F(000)$ = 1856; T = 173(2) K; R_1 = 0.0375, wR^2 = 0.0831, 10028 independent reflections ($2\theta \leq 56.68°$) and 446 parameters.

Crystal data for 10′: $C_{42}H_{52}AlCl_3N_4Pt$; M_r = 941.30; yellow block; 0.37 × 0.40 × 0.56 mm^3; monoclinic; space group $P2_1/c$; a = 13.476(4), b = 13.688(4), c = 22.146(6) Å; α = 90.00, β = 94.185(4), γ = 90.00°; V = 4074(2) Å^3; Z = 4; ρ_{calcd} = 1.535 g cm^{-3}; μ = 3.697 mm^{-1}; $F(000)$ = 1896; T = 172(2) K; R_1 = 0.0226, wR^2 = 0.0482, 10270 independent reflections ($2\theta \leq 57.06°$) and 472 parameters.

CCDC-770521 (**8**), -770647 (**9**), 770648 (**10**), -770649 (**8′**), 770650 (**9′**), and -770651 (**10′**) contain the supplementary crystallographic data for this paper. These data can be obtained free of charge from The Cambridge Crystallographic Data Centre via www.ccdc.cam.ac.uk/data_request/cif.

Acknowledgements

J.B. is grateful to the Fonds der Chemischen Industrie for a Ph.D. fellowship.

[1] D. F. Shriver, *Acc. Chem. Res.* **1970**, *3*, 231–238.
[2] L. Vaska, J. W. DiLuzio, *J. Am. Chem. Soc.* **1961**, *83*, 2784–2785.
[3] M. C. Baird, G. Wilkinson, *Chem. Commun.* **1966**, 267–268.
[4] J. P. Collman, W. R. Roper, *Adv. Organomet. Chem.* **1969**, *7*, 53–94.
[5] J. Halpern, *Acc. Chem. Res.* **1970**, *3*, 386–392.
[6] L. Vaska, *Acc. Chem. Res.* **1968**, *1*, 335–344.
[7] G. Alcaraz, M. Grellier, S. Sabo-Etienne, *Acc. Chem. Res.* **2009**, *42*, 1640–1649.
[8] F. G. Fontaine, J. Boudreau, M. H. Thibault, *Eur. J. Inorg. Chem.* **2008**, 5439–5454.
[9] I. Kuzu, I. Krummenacher, J. Meyer, F. Armbruster, F. Breher, *Dalton Trans.* **2008**, 5836–5865.
[10] R. N. Perutz, S. Sabo-Etienne, *Angew. Chem.* **2007**, *119*, 2630–2645; *Angew. Chem. Int. Ed.* **2007**, *46*, 2578–2592.
[11] H. Werner, *Angew. Chem.* **1983**, *95*, 932–954; *Angew. Chem. Int. Ed. Engl.* **1983**, *22*, 927–949.
[12] F. W. B. Einstein, R. K. Pomeroy, P. Rushman, A. C. Willis, *J. Chem. Soc. Chem. Commun.* **1983**, 854–855.
[13] F. Jiang, J. L. Male, K. Biradha, W. K. Leong, R. K. Pomeroy, M. J. Zaworotko, *Organometallics* **1998**, *17*, 5810–5819.
[14] F. Jiang, H. A. Jenkins, K. Biradha, H. B. Davis, R. K. Pomeroy, M. J. Zaworotko, *Organometallics* **2000**, *19*, 5049–5062.
[15] H. B. Davis, F. W. B. Einstein, P. G. Glavina, T. Jones, R. K. Pomeroy, P. Rushman, *Organometallics* **1989**, *8*, 1030–1039.
[16] R. Usó, J. Fornies, P. Espinet, C. Fortuno, M. Tomas, A. J. Welch, *J. Chem. Soc. Dalton Trans.* **1988**, 3005–3009.
[17] J. T. Golden, T. H. Peterson, P. L. Holland, R. G. Bergman, R. A. Andersen, *J. Am. Chem. Soc.* **1998**, *120*, 223–224.
[18] A. F. Hill, G. R. Owen, A. J. P. White, D. J. Williams, *Angew. Chem.* **1999**, *111*, 2920–2923; *Angew. Chem. Int. Ed.* **1999**, *38*, 2759–2761.
[19] R. J. Blagg, J. P. H. Charmant, N. G. Connelly, M. F. Haddow, A. G. Orpen, *Chem. Commun.* **2006**, 2350–2352.
[20] I. R. Crossley, A. F. Hill, *Organometallics* **2004**, *23*, 5656–5658.
[21] I. R. Crossley, M. R. S. Foreman, A. F. Hill, A. J. P. White, D. J. Williams, *Chem. Commun.* **2005**, 221–223.
[22] I. R. Crossley, A. F. Hill, A. C. Willis, *Organometallics* **2007**, *26*, 3891–3895.
[23] I. R. Crossley, M. R. S. Foreman, A. F. Hill, G. R. Owen, A. J. P. White, D. J. Williams, A. C. Willis, *Organometallics* **2008**, *27*, 381–386.
[24] I. R. Crossley, A. F. Hill, *Dalton Trans.* **2008**, 201–203.
[25] I. R. Crossley, A. F. Hill, A. C. Willis, *Organometallics* **2008**, *27*, 312–315.
[26] V. K. Landry, J. G. Melnick, D. Buccella, K. Pang, J. C. Ulichny, G. Parkin, *Inorg. Chem.* **2006**, *45*, 2588–2597.
[27] D. J. Mihalcik, J. L. White, J. M. Tanski, L. N. Zakharov, G. P. A. Yap, C. D. Incarvito, A. L. Rheingold, D. Rabinovich, *Dalton Trans.* **2004**, 1626–1634.

[28] G. R. Owen, P. Hugh Gould, J. P. H. Charmant, A. Hamilton, S. Saithong, *Dalton Trans.* **2010**, *39*, 392–400.
[29] K. Pang, S. M. Quan, G. Parkin, *Chem. Commun.* **2006**, 5015–5017.
[30] K. Pang, J. M. Tanski, G. Parkin, *Chem. Commun.* **2008**, 1008–1010.
[31] N. Tsoureas, M. F. Haddow, A. Hamilton, G. R. Owen, *Chem. Commun.* **2009**, 2538–2540.
[32] I. R. Crossley, A. F. Hill, A. C. Willis, *Organometallics* **2010**, *29*, 326–336.
[33] M. Sircoglou, S. Bontemps, G. Bouhadir, N. Saffon, K. Miqueu, W. Gu, M. Mercy, C. H. Chen, B. M. Foxman, L. Maron, O. V. Ozerov, D. Bourissou, *J. Am. Chem. Soc.* **2008**, *130*, 16729–16738.
[34] P. Gualco, T. P. Lin, M. Sircoglou, M. Mercy, S. Ladeira, G. Bouhadir, L. M. Perez, A. Amgoune, L. Maron, F. P. Gabbai, D. Bourissou, *Angew. Chem.* **2009**, *121*, 10076–10079; *Angew. Chem. Int. Ed.* **2009**, *48*, 9892–9895.
[35] J. Wagler, A. F. Hill, T. Heine, *Eur. J. Inorg. Chem.* **2008**, 4225–4229.
[36] J. Wagler, E. Brendler, *Angew. Chem.* **2010**, *122*, 634–637; *Angew. Chem. Int. Ed.* **2010**, *49*, 624–627.
[37] S. Bontemps, H. Gornitzka, G. Bouhadir, K. Miqueu, D. Bourissou, *Angew. Chem.* **2006**, *118*, 1641–1644; *Angew. Chem. Int. Ed.* **2006**, *45*, 1611–1614.
[38] S. Bontemps, G. Bouhadir, K. Miqueu, D. Bourissou, *J. Am. Chem. Soc.* **2006**, *128*, 12056–12057.
[39] S. Bontemps, G. Bouhadir, P. W. Dyer, K. Miqueu, D. Bourissou, *Inorg. Chem.* **2007**, *46*, 5149–5151.
[40] S. Bontemps, G. Bouhadir, W. Gu, M. Mercy, C. H. Chen, B. M. Foxman, L. Maron, O. V. Ozerov, D. Bourissou, *Angew. Chem.* **2008**, *120*, 1503–1506; *Angew. Chem. Int. Ed.* **2008**, *47*, 1481–1484.
[41] S. Bontemps, M. Sircoglou, G. Bouhadir, H. Puschmann, J. A. K. Howard, P. W. Dyer, K. Miqueu, D. Bourissou, *Chem. Eur. J.* **2008**, *14*, 731–740.
[42] M. Sircoglou, S. Bontemps, M. Mercy, N. Saffon, M. Takahashi, G. Bouhadir, L. Maron, D. Bourissou, *Angew. Chem.* **2007**, *119*, 8737–8740; *Angew. Chem. Int. Ed.* **2007**, *46*, 8583–8586.
[43] M. Sircoglou, M. Mercy, N. Saffon, Y. Coppel, G. Bouhadir, L. Maron, D. Bourissou, *Angew. Chem.* **2009**, *121*, 3506–3509; *Angew. Chem. Int. Ed.* **2009**, *48*, 3454–3457.
[44] H. Braunschweig, D. Rais, K. Uttinger, *Angew. Chem.* **2005**, *117*, 3829–3832; *Angew. Chem. Int. Ed.* **2005**, *44*, 3763–3766.
[45] H. Braunschweig, K. Radacki, D. Rais, G. R. Whittell, *Angew. Chem.* **2005**, *117*, 1217–1219; *Angew. Chem. Int. Ed.* **2005**, *44*, 1192–1194.
[46] H. Braunschweig, G. R. Whittell, *Chem. Eur. J.* **2005**, *11*, 6128–6133.
[47] H. Braunschweig, K. Radacki, D. Rais, D. Scheschkewitz, *Angew. Chem.* **2005**, *117*, 5796–5799; *Angew. Chem. Int. Ed.* **2005**, *44*, 5651–5654.
[48] H. Braunschweig, K. Radacki, D. Rais, F. Seeler, *Angew. Chem.* **2006**, *118*, 1087–1090; *Angew. Chem. Int. Ed.* **2006**, *45*, 1066–1069.
[49] H. Braunschweig, K. Radacki, D. Rais, K. Uttinger, *Organometallics* **2006**, *25*, 5159–5164.
[50] H. Braunschweig, C. Burschka, M. Burzler, S. Metz, K. Radacki, *Angew. Chem.* **2006**, *118*, 4458–4461; *Angew. Chem. Int. Ed.* **2006**, *45*, 4352–4355.
[51] H. Braunschweig, K. Radacki, K. Uttinger, *Eur. J. Inorg. Chem.* **2007**, 4350–4356.
[52] H. Braunschweig, M. Burzler, R. D. Dewhurst, K. Radacki, F. Seeler, *Z. Anorg. Allg. Chem.* **2008**, *634*, 1875–1879.
[53] J. M. Mayer, J. C. Calabrese, *Organometallics* **1984**, *3*, 1292–1298.
[54] H. Braunschweig, K. Gruss, K. Radacki, *Angew. Chem.* **2007**, *119*, 7929–7931; *Angew. Chem. Int. Ed.* **2007**, *46*, 7782–7784.
[55] H. Braunschweig, K. Gruss, K. Radacki, *Inorg. Chem.* **2008**, *47*, 8595–8597.
[56] H. Braunschweig, K. Gruss, K. Radacki, *Angew. Chem.* **2009**, *121*, 4303–4305; *Angew. Chem. Int. Ed.* **2009**, *48*, 4239–4241.
[57] H. Braunschweig, K. Radacki, K. Schwab, *Chem. Commun.* **2010**, *46*, 913–915.
[58] S. Diez-Gonzalez, N. Marion, S. P. Nolan, *Chem. Rev.* **2009**, *109*, 3612–3676.
[59] W. A. Herrmann, *Angew. Chem.* **2002**, *114*, 1342–1363; *Angew. Chem. Int. Ed.* **2002**, *41*, 1290–1309.
[60] H. Jacobsen, A. Correa, A. Poater, C. Costabile, L. Cavallo, *Coord. Chem. Rev.* **2009**, *253*, 687–703.
[61] M. Scholl, S. Ding, C. W. Lee, R. H. Grubbs, *Org. Lett.* **1999**, *1*, 953–956.
[62] R. A. Kelly III, H. Clavier, S. Giudice, N. M. Scott, E. D. Stevens, J. Bordner, I. Samardjiev, C. D. Hoff, L. Cavallo, S. P. Nolan, *Organometallics* **2008**, *27*, 202–210.
[63] H. Clavier, S. P. Nolan, *Chem. Commun.* **2010**, *46*, 841–861.
[64] S. Otsuka, T. Yoshida, M. Matsumoto, K. Nakatsu, *J. Am. Chem. Soc.* **1976**, *98*, 5850–5858.
[65] A. Immirzi, A. Musco, P. Zambelli, G. Carturan, *Inorg. Chim. Acta* **1975**, *13*, L13L14.
[66] A. Immirzi, A. Musco, *J. Chem. Soc. Chem. Commun.* **1974**, 400–401.
[67] S. Fantasia, S. P. Nolan, *Chem. Eur. J.* **2008**, *14*, 6987–6993.
[68] P. Parameswaran, G. Frenking, *J. Phys. Chem. A* **2010**, *114*, 8529–8535
[69] H. Lew, G. Wessel, *Phys. Rev.* **1953**, *90*, 1–3.
[70] H. Braunschweig, K. Radacki, K. Uttinger, *Chem. Eur. J.* **2008**, *14*, 7858–7866.
[71] All details for computational results see the Supporting Information.
[72] A. E. Reed, R. B. Weinstock, F. Weinhold, *J. Chem. Phys.* **1985**, *83*, 735–746.
[73] A. E. Reed, F. Weinhold, *J. Chem. Phys.* **1985**, *83*, 1736–1740.
[74] A. E. Reed, L. A. Curtiss, F. Weinhold, *Chem. Rev.* **1988**, *88*, 899–926.
[75] J. P. Foster, F. Weinhold, *J. Am. Chem. Soc.* **1980**, *102*, 7211–7218.
[76] D. Nemcsok, K. Wichmann, G. Frenking, *Organometallics* **2004**, *23*, 3640–3646.
[77] M. D. Sanderson, J. W. Kamplain, C. W. Bielawski, *J. Am. Chem. Soc.* **2006**, *128*, 16514–16515.
[78] G. M. Sheldrick, *Acta Crystallogr. Sect. A* **2008**, *64*, 112–122.

Received: May 7, 2010
Published online: September 10, 2010

